Journal of Molecular Structure 1086 (2015) 179–189

Contents lists available at ScienceDirect

Journal of Molecular Structure

journal homepage: www.elsevier.com/locate/molstruc

Synthesis and characterization of *n*-alkylamino derivatives of vitamin K3: Molecular structure of 2-propylamino-3-methyl-1,4-naphthoquinone and antibacterial activities

Dattatray Chadar [a], Maria Camilles [a], Rishikesh Patil [a], Ayesha Khan [a], Thomas Weyhermüller [b], Sunita Salunke-Gawali [a,*]

[a] Department of Chemistry, Savitribai Phule Pune University, Pune 411007, India
[b] MPI für Chemische Energiekonversion, Stiftstr. 34-36, 45470 Mülheim an der Ruhr, Germany

HIGHLIGHTS

- First eight *n*-alkylamino derivatives of vitamin K3 were synthesized.
- There were four molecules in asymmetric unit cell of propyl derivative.
- No molecular interaction between molecules I and II similarly III and IV.
- Molecules I, III and II, IV showed C—H···O and π–π stacking interactions.
- All compounds are active against *Pseudomonas aeruginosa* and *Staphylococcus aureus*.

GRAPHICAL ABSTRACT

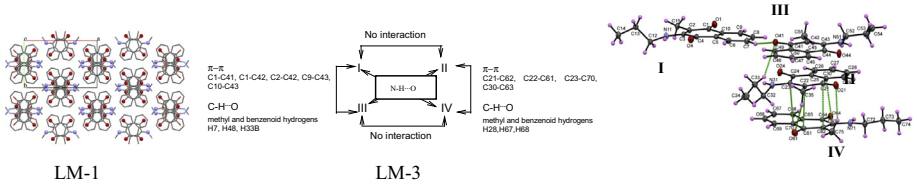

LM-1 LM-3

ARTICLE INFO

Article history:
Received 20 October 2014
Received in revised form 14 January 2015
Accepted 15 January 2015
Available online 27 January 2015

Keywords:
Menadione
Vitamin K3
Naphthoquinone
π–π stacking
Hydrogen bonding
Michael addition

ABSTRACT

We would like to introduce eight analogues of *n*-alkylamino derivatives of vitamin K3 (2-methyl-1,4-naphthoquinone) viz, 2-(*n*-alkylamino)-3-methyl-1,4-naphthoquinone (where *n*-alkyl is methyl; LM-1, ethyl; LM-2, propyl; LM-3, butyl; LM-4, pentyl; LM-5, hexyl; LM-6, heptyl; LM-7, octyl; LM-8). All the above analogues have been successfully synthesized from vitamin K3 and characterized using different analytical techniques. Furthermore, in order to understand the mechanistic aspects of formation of LM-1 to LM-8 compounds, we could propose the mechanism. The FT-IR analysis of LM-1 to LM-8 indicate the presence of characteristic band of N—H group ~3287–3364 cm^{-1}, the variation was attributed to extensive intramolecular hydrogen bonding interaction. The molecular structure of LM-3 compound has been confirmed by single crystal X-ray diffraction analysis. LM-3 compound crystallises in triclinic space group *P*1. There were four independent molecules in asymmetric unit cell and their molecular interactions observed via N—H···O, C—H···O and π–π stacking of quinonoid rings. Pharmacological potential of all compounds has been evaluated in terms of their antibacterial activities against *Pseudomonas aeruginosa* and *Staphylococcus aureus*. All the compounds were active against both the strains while LM-2 was found to be more effective with a minimum inhibition concentration of 0.3125 μg/mL and 0.156 μg/mL respectively.

* Corresponding author. Tel.: +91 2025601397x531; fax: +91 2025693981.
E-mail address: sunitas@chem.unipune.ac.in (S. Salunke-Gawali).

http://dx.doi.org/10.1016/j.molstruc.2015.01.029
0022-2860/

Introduction

Vitamin K is a group of structurally similar and fat-soluble vitamins that are needed for the post-translational modification of certain proteins required for blood coagulation as well as in metabolic pathways in bone and other tissues. Vitamin K is found chiefly in green leafy vegetables such as dandelion greens, spinach, swiss chard and *Brassica* (*e.g.* Cabbage, cauliflower, broccoli and brussel sprouts). Some fruits, such as avocado, kiwifruit and grapes are also high in vitamin K. Colonic bacteria synthesize a significant portion of vitamin K that needs human. The potential health problems that can be associated with vitamin K deficiency include arterial calcification, cardiovascular disease and varicose veins, osteoporosis, prostate cancer, lung cancer, liver cancer and leukemia, brain health problems, including dementia, tooth decay and infectious diseases like pneumonia.

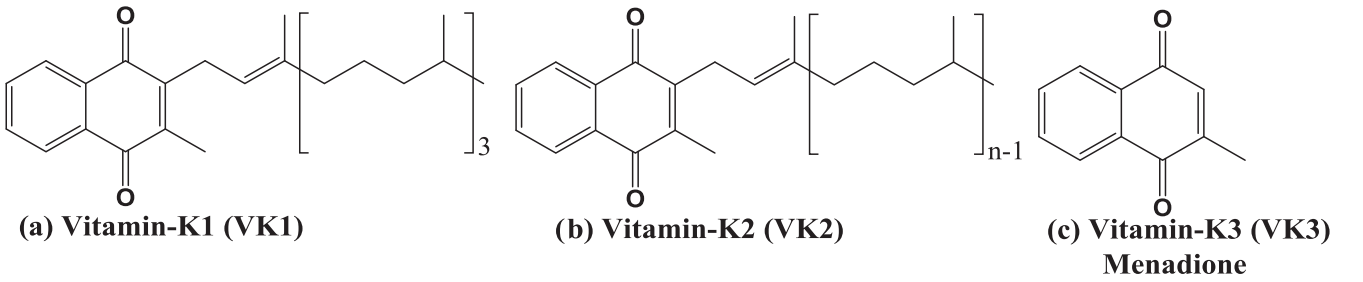

All form of vitamin K share a common scaffold viz. 1,4-naphthoquinone ring, however differ in the C(3) side chain. There are three major types of vitamin K, phylloquinone (VK1), menaquinone (VK2) and menadione (VK3). VK1 and VK2 are the natural compounds; the most common form of VK2 in human is menaquinone-4 (MK-4) [1]. VK3 (2-methyl-1,4-naphthoquinone) is considered as the synthetic analogue. Davidson et al. [2–4] have found that dietary VK1 can be cleaved to form VK3 by bacteria present in the intestine. It is also an intermediate metabolite in the conversion of VK1 to MK4 [5] and plays important role in blood coagulation as a cofactor for the synthesis of clotting factors in liver and in bone mineralisation [4,6].

Biological activity of quinones has been related to their capacity to accept one or two electrons to forms the corresponding radical anion or radical dianion. The electron uptake capacity of a given quinone can be modified by directly adding substituent's to the quinone structure. Structural aspects are very important factor as for as the biological activity of the synthetic molecules are concerned. We have described in our series of reports on the *n*-alkylaminno derivatives of naphthoquinones, that these molecules could provide facile sites for molecular interaction to biomolecules. These interactions could include hydrogen bonding, π–π stacking interactions [7]. Our main interest in the resent years is to study the molecular interactions of *n*-alkylaminno derivatives of naphthoquinones by single crystal X-ray diffraction and to correlate their structural features with the biological activity. In the present investigation, we have reported the detailed synthesis and characterization of *n*-alkylamino derivatives of vitamin K3 (Scheme 1). As there is great pharmacological potential for such compounds [8] more systematic studies have been made with respect to characterization of these derivatives in the present investigation. The antibacterial activities of these compounds were also evaluated against two bacterial strains namely viz., *Staphylococcus aureus* and *Pseudomonas aeruginosa*.

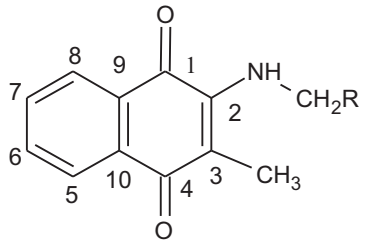

Scheme 1. Molecular formula of LM-1 to LM-8. Where, LM-1: R=H; LM-2: R=CH_3; LM-3:R=C_2H_5, LM-4: R=C_3H_7, LM-5: R=C_4H_9; LM-6: R=C_5H_{11}; LM-7: R=C_6H_{13}; LM-8: R=C_7H_{15}.

Experimental section

General materials and methods

The materials used viz., 2-methyl-1,4-naphthoquinone, methyl amine solution (40%), ethyl amine solution (70%), propyl, butyl, pentyl, hexyl, heptyl and octyl amine were purchased from Sigma–Aldrich and used as received. Analytical grade solvents used such as dichloromethane, toluene, methanol were purchased from Merck Chemicals. Solvents were distilled by standard methods [9] and dried wherever necessary. FT-IR spectra were recorded between 4000 and 400 cm^{-1} as KBr pellets on SHIMADZU FT 8400 Spectrophotometer (Fig. S1a–h in ESI†). Melting points of LM-1 to LM-8 were determined using (Make-METTLER) and were corrected using DSC (Differential Scanning Calorimetry) technique (Make-TA Q2000) (Fig. S2a–h in ESI†). ^1H, ^{13}C and DEPT NMR of compounds were recorded (Fig. S3a–h and Table S1 in ESI†) in DMSO-d_6, on Varian 500 MHz NMR instrument. TMS (tetramethylsilane) was used as the reference. Elemental analysis was performed on Thermo Finnigan EA 1112 Flash series Elemental Analyzer and on Elementar Vario EL III. Mass of LM-1 to LM-8 was determined by GC–MS 2010-eV (Make SHIMADZU).

Synthesis

Synthesis of n-alkylamino derivatives of vitamin K3

1 g of vitamin K3 (5.80 mM) was taken in a two necked round bottom flask. About 25 ml dichloromethane was added to it just so that it dissolves. After stirring the solution on a magnetic stirrer

Table 1
Details of concentration of primary amines used in synthesis of LM-1 to LM-8.

Comp.	Vitamin K3 weight (g)	Primary amine (% sol^n)	Density g/cm^3	Volume mL	Yield (%)
LM-1	1.0	Methyl (40%)	0.893	0.504	42.40
LM-2	1.0	Ethyl (70%)	0.800	0.543	40.00
LM-3	1.0	Propyl (99%)	0.717	0.482	38.72
LM-4	1.0	Butyl (99%)	0.740	0.571	37.31
LM-5	1.0	Pentyl (99%)	0.752	0.772	39.66
LM-6	1.0	Hexyl (99%)	0.766	0.772	32.33
LM-7	1.0	Heptyl (99%)	0.777	0.861	34.50
LM-8	1.0	Octyl (99%)	0.782	0.950	34.28

for about 15 min, calculated amount of primary amine solution (Table 1) (methylamine, ethylamine, propylamine, butylamine, amylamine, hexylamine, heptylamine, octylamine) was added to it. The reaction was kept for 24 h with constant stirring at room temperature ~28 °C. During this time the progress of the reaction was monitored using thin layer chromatography. After 24 h the mixture was transferred to a beaker and kept for another 24 h for the solvent to evaporate. The solid crude product was obtained by evaporation. The crude product was purified by column chromatography using toluene: methanol (9:1) as eluent. Red colour needles of all the derivatives were obtained by the slow evaporation of eluent.

Characterization of 2-ethylamino-3-methyl-1,4-naphthoquinone (LM-2)

Dark red crystal, Yield: 0.499 g (40.0%). M. P. 87.97 °C. Anal. data calcd. for $C_{13}H_{13}NO_2$ C, 71.63; H, 5.51; N, 6.96. Found: C, 72.29; H, 6.20; N, 6.51. FT-IR (ν_{max}/cm^{-1}): 3285, 3182, 3068, 2966, 2926, 2870, 1670, 1602, 1566, 1510, 1452, 1344, 1280, 1228, 1184, 1150, 1080, 1051, 1028, 979, 941, 887, 862, 804, 725, 684, 630, 553, 518, 478, 435, 410. ^{1}H NMR (500 MHz, DMSO-d_6, δ/ppm): 1.15 (t, 3H, J = 7.00 Hz), 3.55 (p, 2H, J = 7.00 Hz), 6.56 (br. S, 1H, D_20 ex.), 2.07 (s, 3H), 7.65 (t, 1H, J = 7.50 Hz), 7.75 (t, 1H, J = 7.90 Hz), 7.88 (d, 1H, J = 7.80 Hz), 7.90 (d, 1H, J = 8.60 Hz). UV–Vis (λ_{max}/nm, DMSO): 280, 313, 486. GC–MS (m/z): 215 (M^+ + H).

Characterization of 2-propylamino-3-methyl-1,4-naphthoquinone (LM-3)

Red crystals, Yield: 0.515 g (38.72%). M. P. 77.19 °C. Anal. data calcd. for $C_{14}H_{15}NO_2$: C, 73.34; H, 6.59; N, 6.11. Found: C, 73.03; H, 6.50; N, 5.64. FT-IR (KBr, ν_{max}/cm^{-1}): 3284, 3180, 3068, 2958, 2872, 1669, 1602, 1566, 1510, 1452, 1344, 1280, 1228, 1184, 1151, 1099, 1080, 1060, 1026, 976, 896, 786, 727, 684, 630,557, 503, 451, 441. ^{1}H NMR (500 MHz, DMSO-d_6, δ/ppm): 0.83 (t, 3H, J = 7.50 Hz), 1.55 (p, 2H, J = 7.75 Hz), 3.41 (q, 2H, J = 7.20 Hz), 2.03 (s, 3H), 6.53 (br. 1H), 7.69 (t, 1H, J = 7.50 Hz), 7.80 (t, 1H, J = 7.50 Hz), 7.84 (d, 1H, J = 7.25 Hz), 7.90 (d, 1H, J = 7.75 Hz). UV–Vis (λ_{max}/nm, DMSO): 281, 339, 487. GC–MS (EI); m/z: 229 (M^+ + H).

Characterization of 2-pentylamino-3-methyl-1,4-naphthoquinone (LM-5)

Red crystal, Yield: 0.591 g (39.66%). M. P. 83.31 °C. Anal. data calcd. for $C_{16}H_{19}NO_2$: C, 74.68; H, 7.44; N, 5.44. Found: C, 74.71; H, 7.55; N, 5.66. FT-IR (KBr, ν_{max}/cm^{-1}): 3338, 33072, 2952, 2866, 1668, 1601, 1565, 1525, 1462, 1340, 1301, 1274, 1230, 1180, 1155, 1087, 1064, 1026, 985, 906, 840, 792, 729, 688, 636, 555, 505, 457,428. ^{1}H NMR (500 MHz, DMSO-d_6, δ/ppm): 0.82 (t, 3H, J = 7.80 Hz), 1.25 (m, 2H, J = 7.20), 1.52 (p, 2H, J = 7.20 Hz), 3.49 (q, 2H, J = 7.00 Hz), 2.08 (s, 3H), 6.53 (br. 1H), 7.64 (t, 1H, J = 7.25 Hz), 7.74 (t, 1H, J = 7.25 Hz), 7.88 (d, 1H, J = 7.25 Hz), 7.90 (d, 1H, J = 7.80 Hz). UV–Vis; (λ_{max}/nm, DMSO): 280, 335, 487. GC–MS (EI); m/z: 257 (M^+ + H).

Characterization of 2-heptylamino-3-methyl-1,4-naphthoquinone (LM-7)

Red crystal, Yield: 0.568 g (34.5%). M. P. 51.42 °C. Anal. data calcd. for $C_{18}H_{23}NO_2$: C, 75.76; H, 8.12; N, 4.91. Found: C, 75.21; H, 8.04; N, 5.21. FT-IR (KBr, ν_{max}/cm^{-1}): 3323, 3066, 2955, 2924, 2856, 1668, 1599, 1564, 1510, 1460, 1334, 1300, 1278, 1230, 1180, 1153, 1085, 1030, 970, 893, 800, 767, 727, 684, 653, 623, 561, 507, 451, 418. ^{1}H NMR (500 MHz, DMSO-d_6, δ/ppm): 0.83 (t, 3H, J = 7.00 Hz), 1.25 (m, 2H, J = 7.25 Hz)), 1.55 (p, 2H, J = 7.25 Hz), 3.35 (q, 2H, J = 7.00 Hz), 2.07 (s, 3H), 6.59 (br. 1H), 7.66 (t, 1H, J = 7.50 Hz), 7.75 (t, 1H, J = 7.75 Hz), 7.84 (d, 1H, J = 7.25 Hz), 7.99 (d, 1H, J = 7.75 Hz). UV–Vis (λ_{max}/nm, DMSO): 281, 342, 487. GC–MS (EI); m/z: 285 (M^+ + H).

Characterization of 2-octylamino-3-methyl-1,4-naphthoquinone (LM-8)

Red crystal, Yield: 0.593 g (34.28%). M. P. 60.96 °C. Anal. data calcd. for $C_{19}H_{25}NO_2$: C, 76.27; H, 8.42; N, 4.68. Found: C, 76.28; H, 7.77; N, 4.83. FT-IR (KBr, ν_{max}/cm^{-1}): 3282, 3068, 2958, 2922, 2853, 1668, 1618, 1600, 1566, 1505, 1457, 1366, 1339, 1300, 1277, 1233, 1179, 1157, 1124, 1107, 1083, 1063, 1028, 969, 952, 896, 813, 797, 753, 724, 683, 667, 652, 623, 561, 532, 509, 470, 453, 434, 411. ^{1}H NMR (500 MHz, DMSO-d_6, δ/ppm): 0.82 (t, 3H, J = 7.00 Hz), 1.25 (m, 2H, 7.25), 3.51 (q, 2H, J = 7.80 Hz), 2.05 (s, 3H), 6.60 (br. 1H), 7.67 (t, 1H, J = 7.50 Hz), 7.76 (t, 1H, J = 7.25 Hz), 7.86 (d, 1H, J = 7.75 Hz), 7.92 (d, 1H, J = 8.00 Hz). UV–Vis (λ_{max}/nm, DMSO): 280, 340, 487. GC–MS (EI); m/z: 299 (M^+ + H).

X-ray crystallographic data collection and refinement of the structure

Single crystals of LM-3 was coated with perfluoropolyether, picked up with nylon loops and was mounted in the nitrogen cold stream of the diffractometer. Monochromated Mo Kα radiation (Bruker-AXS Kappa Mach3 with Incoatec Helios mirror, λ = 0.71073 Å) from a Mo-target rotating-anode X-ray source was used for LM-3. Final cell constants were obtained from least squares fits of several thousand strong reflections. Intensity data were corrected for absorption using intensities of redundant reflections with the program SADABS [10]. The structures were readily solved by direct methods and subsequent difference Fourier techniques. The Siemens ShelXTL [11] software package was used for solution and artwork of the structures, ShelXL97 [12] was used for the refinement. All non-hydrogen atoms were anisotropically refined and hydrogen atoms were placed at calculated positions

Table 2
Crystal data and structure refinement for LM-3.

Identification code	LM-3
Empirical formula	$C_{14}H_{15}NO_2$
Formula weight	229.27
Temperature	100(2) K
Wavelength	0.71073 A
Crystal system, space group	Triclinic, P1
Unit cell dimensions	a = 9.8975(6) Å α = 97.904(4)°
	b = 9.9631(6) Å β = 107.789(5)°
	c = 12.7937(8) Å γ = 100.155(4)°
Z, Calculated density	4, 1.316 Mg/m^3
Absorption coefficient	0.088 mm^{-1}
F(000)	488
Crystal size	0.16 × 0.16 × 0.10 mm
Theta range for data collection	2.69–33.09°
Limiting indices	$-15 \leqslant h \leqslant 13$, $-15 \leqslant k \leqslant 15$, $-19 \leqslant l \leqslant 19$
Reflections collected/unique	31,985/16,066 [R(int) = 0.0534]
Completeness to theta	33.09% and 99.7%
Max. and min. transmission	0.99206 and 0.98593
Refinement method	Full-matrix least-squares on F^2
Data/restraints/parameters	16,066/3/633
Goodness-of-fit on F^2	1.070
Final R indices [I > 2sigma(I)]	$R1$ = 0.0569, $wR2$ = 0.1176
R indices (all data)	$R1$ = 0.0852, $wR2$ = 0.1327
Absolute structure parameter	Not applicable, light atom structure
Largest diff. peak and hole	0.397 and −0.330 e Å^{-3}

and refined as riding atoms with isotropic displacement parameters. Crystallographic data of the compounds are listed in Table 2.

Antibacterial activity

Agar disc diffusion assay

Bacterial strains *P. aeruginosa* (PAO-1) and *S. aureus* were obtained for National Chemical Laboratory, Pune, India. Initially, the apparatus as well as potato dextrose agar (PDA) (5.85 g in 150 ml distilled water) was sterilized by autoclaving it for 20 min. The PDA was then poured on to the petri plates and kept for 24 h. The work was carried out in the laminar air flow (Microfilt) using a micropipette 200 μL of bacterial sample was spread on to the plates evenly using a spreader. Using sterilized forceps small sterilized discs of Whatman filter paper 1 was placed on the plate equidistantly. On these discs 1 μL, 2 μL, 3 μL and 5 μL of the compounds LM-1 to LM-8 and vitamin K3 solutions in DMSO were placed (Concentration of the compound = 2 mg/100 μL.). DMSO was used as a control. The plates were then incubated at 30 °C for 48 h and the zone of inhibitions were measured.

Minimum inhibitory concentration assay (MIC)

Using a multipipettor, 100 μL of medium was dispensed into the wells of a microtitre plate. The plates and lid were labelled. About 100 μL of appropriate 2× antibiotic solutions were pipetted into the wells in column 1. Using the multipipette set at 100 μL, the antibiotics were mixed into the wells of column 1 by sucking up and down 6–7 times. 100 μL mixtures were withdrawn from column 1, and added this to column 2. This made column 2 a twofold dilution of column 1 and it was repeated from column 2 to column 3 and so on. The plates were further incubated at 30 °C and latter scanned at 620 nm using a multiplate reader. The results were presented in the form of plots of absorbance Vs concentrations.

Result and discussion

The first eight *n*-alkylamino analogues of vitamin K3 has been synthesized at room temperature (26 °C). The products were obtained by evaporation of dark red fraction from the column. First yellow fraction was found to be unreacted vitamin K3. A dark brown coloured product band retained on the column, which was inseparable by the chromatographic conditions used for separation (9:1, toluene: methanol). The dark red coloured product was later found to be 2-(*n*-alkylamino)-3-methyl-1,4-naphthoquinone with yield of ~40%, which was on the lower side when compared to bromo chloro, hydro derivatives of 2-X-3-(*n*-alkylamino)-1,4-naphthoquinone.

The mechanism for formation of *n*-alkylamino derivatives of vitamin K3 is as shown in Scheme 2. PATH 1 explains the formation of desired product 2-(*n*-alkylamino)-3-methyl-1,4-naphthoquinone, whereas PATH-2 explains formation of the by product. 2-methyl-1,4-naphthoquinone(1), the starting material used in the synthesis is an unsymmetrical Michael acceptor molecule, which could undergo the Michael addition reaction with variety of amines to gives the nucleophilic substitution reaction [13] at the sp^2 carbon atom. As a result, the compound (4) is possibly the major product in this reaction. Mechanistically, it is predicted, that Michael addition of primary amine (1) will lead to the generation of an intermediate compound (3). It could be better represented by enolisation of the compound (3) into the more stable (3′) form.

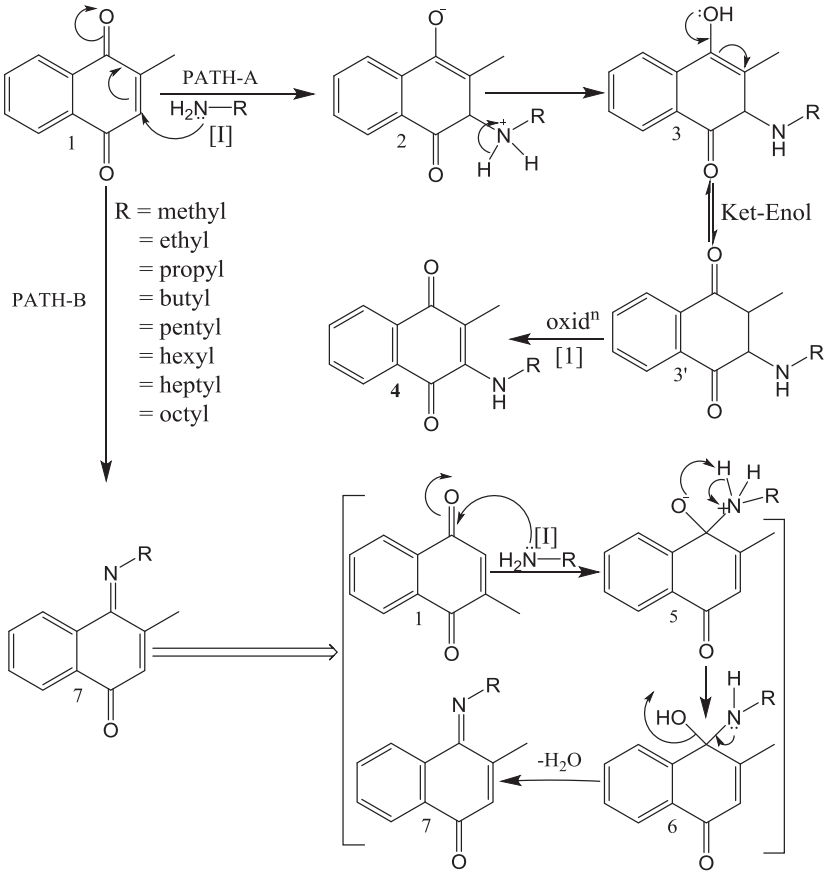

Scheme 2. Probable reaction mechanism of LM-1 to LM-8.

It could undergo oxidation under the influence of another mole of 2-methyl-1,4-naphthoquinone (1) as mentioned by Ji et al. [14]. However, the formation of product (7) is much straight forward, wherein the direct 1,2-addition of the primary amine (I) to vitamin K3 (1) leads to an intermediate (5) as an unstable moiety, which immediately loses the water molecules to give the aminonaphthoquinone (7).

FT-IR studies of LM-1 to LM-8

The band observed ~3364–3282 cm^{-1} in FT-IR spectra of LM-1 to LM-8 was assigned for ν_{N-H} stretching frequency in Fig. 1 (Table 3). The minor variation in ν_{N-H} frequency suggests that it was influenced by intra as well as intermolecular hydrogen bonding especially in LM-2, LM-3 and LM-8. However, it can be generalised that the ν_{N-H} stretch (in LM-1 to LM-8) was observed at a higher frequency as compared to the corresponding chloro, bromo derivatives of 2-(X)-3-(*n*-alkylamino)-1,4-naphthoquinone (L-1 to L-4, L-1Br to L-4Br, and LH-1 to LH-7) [7]. The carbonyl stretching frequency was observed at 1661 cm^{-1} for parent 2-methyl-1,4-napthoquinone, however this frequency was shifted to higher wave number in LM-1 to LM-8. The frequencies were observed in the range of ~1661–1669 cm^{-1} (Fig. 1b). New band appeared at ~1734 cm^{-1} which was also assigned to carbonyl frequency. ν_{C-N} frequency was observed at ~1600 ± 3 cm^{-1}. $\nu_{C=C}$ showed (~1560 cm^{-1}) decrease in frequency to all compounds ~25 cm^{-1} when compared with parent, vitamin K3. Paranaphthoquinone vibrations (ν_{p-NQ}) was observed at ~1280 cm^{-1} and are at lower values than that of vitamin K3, which implies that the carbonyl oxygen are involved in hydrogen bonding.

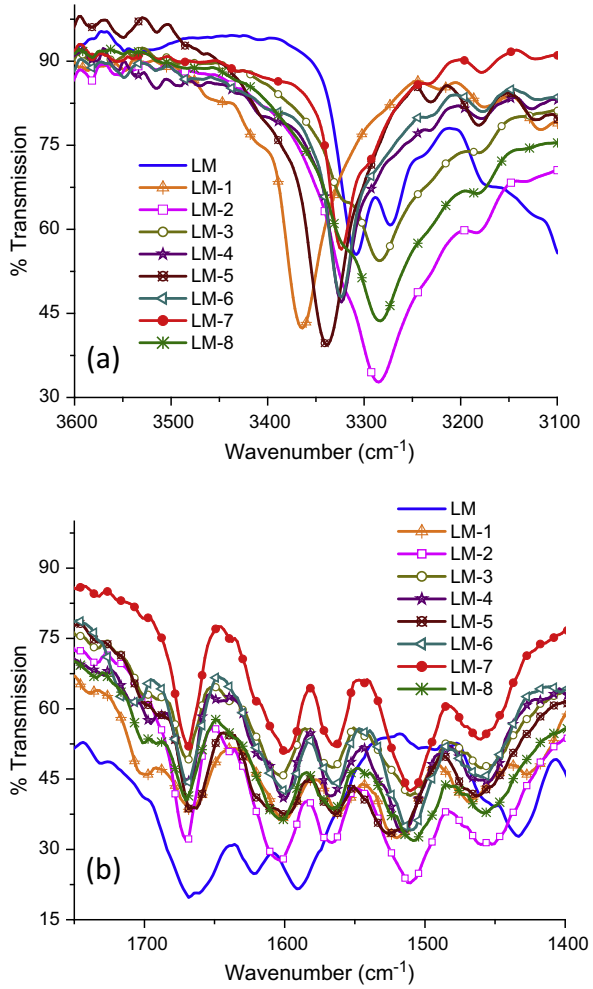

Fig. 1. Characteristic FT-IR frequencies of LM-1 to LM-8 (a) ν_{N-H} region, (b) $\nu_{C=O}$ and ν_{C-N} region.

^{1}H and ^{13}C NMR of LM-1 to LM-8

^{1}H and ^{13}C NMR spectra of the LM-1 to LM-8 were recorded in DMSO-d_6 solvent. In ^{1}H NMR spectra, the terminal methyl protons (a) shows triplet in LM-2 to LM-8, while they are observed as a doublet in LM-1 (Scheme 3). CH_2 protons (h) in LM-3 to LM-8 showed quartet while in LM-2, they are observed as pentet, CH_2 protons (b) in LM-3 to LM-8 showed multiplet. The respective CH_2 protons c, d, e, f and g showed pentet, the resonance of —N(11)—H(11) proton was observed as quartet in LM-1, whereas they observed a triplet in LM-2 to LM-8 ~ δ = 6.59 ppm. ^{13}C chemical shifts were assigned to all compounds and are presented in Table 4.

UV–Visible spectra of LM-1 to LM-8

Electronic spectra of all compounds are shown in Fig. 2. ~1×10^{-4} M concentration were used to record the electronic spectra of LM-1 to LM-8 and the starting material vitamin K3. The absorption of the visible region was observed in starting all compounds owing to a fully conjugated cyclic dione system and the non bonding electrons of the amino group which allows the possibility of n–π* transition in the visible region [7].

The electronic spectra of LM-1 to LM-8 showed the band in the UV region around 291–297 nm and at 335–337 nm (π–π* electronic transition) (Fig. 2). In addition, a third lower energy transition appeared in the visible region of 477 nm. This absorption is typical of amino substituted quinone [15]. The lower energy absorption 477 nm was assigned, to the charge transfer (CT) transition and weak n → π* transition's band result from the electron donating effect of the substituted amine in LM-1 to LM-8. It is known that full delocalization of the nitrogen lone pair requires its orthogonality to be in the plane of naphthoquinone. Thus the shape of the amine influences the extent of the bathochromic shift. LM-1 to LM-8 differed in the length of the alkyl chain present on

Table 3
FT-IR frequencies for vitamin K3 and LM-1 to LM-8.

Comp.	ν_{N-H}	ν_{C-H}	$\nu_{C=O}$	ν_{C-N}	$\nu_{C=C}$	ν_{p-NQ}
LM	–	3068, 2920, 1460, 1156	1660, 1622	–	1590, 1326	1299
LM-1	3364	3072, 3032, 1468, 1158	1667	1600	1562, 1342	1292
LM-2	3285	3182, 3068, 1452, 1150	1670	1602	1510, 1344	1280
LM-3	3284	3180, 3068, 1452, 1151	1669	1602	1566, 1344	1280,
LM-4	3323	3068, 2956, 1454, 1155	1668	1599	1568, 1342	1280
LM-5	3338	2952, 2929, 1462, 1155	1668	1601	1565, 1340	1274
LM-6	3323	3066, 2953, 1459, 1153	1671	1599	1565, 1340	1276
LM-7	3323	3066, 2955, 1460, 1153	1668	1599	1564, 1334	1278
LM-8	3282	3068, 2958, 1458, 1151	1670	1601	1566, 1344	1280

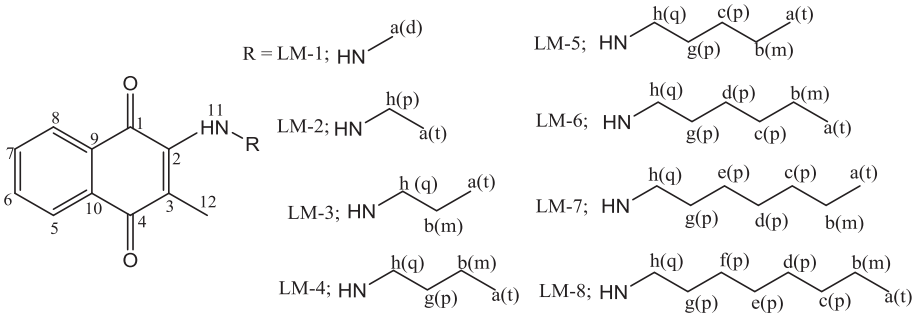

Scheme 3. Atom numbering scheme to assign ^{1}H and ^{13}C NMR spectra of LM-1 to LM-8 (letter a, b, c, d, e, f, g and h are assigned to carbon atom. In parenthesis d (doublet), m (multiplet), p (pentet), q (quartet) and t (triplet) denotes peak obtained in ^{1}H NMR spectra.

Table 4
^{13}C chemical shift (δ/ppm) of LM-1 to LM-8 in DMSO-d_6.

	LM-1	LM-2	LM-3	LM-4	LM-5	LM-6	LM-7	LM-8
C1	181.53	181.54	181.63	181.45	181.55	181.82	181.73	181.56
C2	147.56	146.53	146.71	146.50	146.62	146.90	146.78	146.65
C3	109.89	110.42	110.67	110.49	110.54	110.83	110.72	110.59
C4	182.22	182.19	182.26	182.09	182.22	182.49	182.34	182.24
C5	126.89	125.53	125.36	126.67	125.59	125.85	125.70	125.59
C8	126.23	125.30	125.61	125.48	125.35	125.62	125.46	125.35
C6	134.53	134.34	134.43	134.53	134.41	134.67	134.54	134.78
C7	134.22	132.74	132.78	132.10	132.05	132.17	132.18	132.05
C9	130.71	130.23	130.26	130.12	130.24	130.51	130.32	130.26
C10	131.96	131.99	132.43	131.92	132.77	132.31	132.86	132.78
C-12	10.44	10.51	10.61	10.52	10.61	10.63	10.69	10.63
f	–	–		–	–	–	–	26.10
e	–	–	–	–	–	–	26.14	28.67
d	–	–	–	–	–	26.06	28.44	28.62
c	–	–	–	–	28.35	30.95	31.26	31.20
g	–	–	–	32.65	30.33	30.60	30.66	30.58
b	–	–	23.87	19.28	21.86	22.05	22.08	22.08
h	–	40.26	46.09	44.03	44.39	44.68	44.52	44.41
a	32.40	16.31	11.00	13.60	13.90	13.87	13.99	13.93

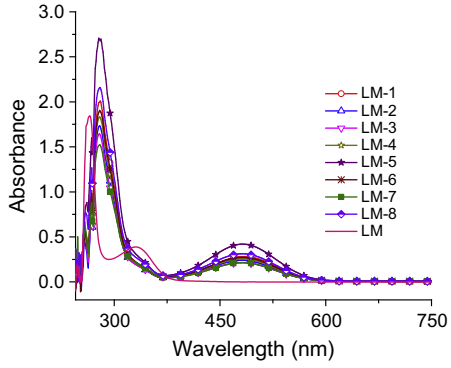

Fig. 2. UV–Visible spectra of vitamin K3 and LM-1 to LM-8 in DMSO with concentration ~1×10^{-4} M.

the amino nitrogen and, therefore, does not differ greatly in their absorption [16–18].

Single crystal X-ray studies of LM-3 and hydrogen bonding interaction of LM-1

Molecules of LM-3 crystallize in triclinic *P*1 space group. There were four independent molecules in asymmetric unit cell. For our convenience we named these molecules as I, II, III and IV, ORTEP diagram of the same shown in Fig. 3 and the crystallographic data were presented in Table 2.

There were minor variation in C=O, C—N bond distances of all four molecules, however all the molecules are in oxidized form unlike other *n*-alkylamino derivatives [7,19] and several other derivatives of vitamin K3 [20]. Major differences were observed to the (i) torsion angles of all four molecules, especially to the plane of quinonoid ring and the N-alkyl groups (Table S2 in ESI†) and similarly (ii) bond angle especially ∠N(11)—C(12)—C(13) and ∠N(31)—C(32)—C(33) are 114.3°, while ∠N(51)—C(52)—C(53) = 110.3° and ∠N(71)—C(72)—C(73) = 109.3°.

Molecules of LM-3 show intra as well as intermolecular hydrogen bonding (Table 5). Among four molecules of LM-3, similar ends of pair of molecule I, IV and II, III formed dimers via N—H···O interactions. However D···A distances as well as ∠D—H···A varies in these dimers (Table 5).

Molecules I, III and II, IV showed π–π stacking as well as C—H···O interaction of benzenoid ring hydrogen's (Fig. 4). The carbon atoms involved in π–π stacking interaction of molecules I and III are C(1)···C(41) (3.361(3) Å), C(1)···C(42) (3.319(3) Å), C(2)···C(41) (3.300(3) Å), C(9)···C(43) (3.466(3) Å), C(10)···C(43) (3.362(2) Å) (1 + *x*,*y*,*z*), and those of molecules II and IV are C(21)···C(62) (3.299(3) Å), C(22)···C(61) (3.299(3) Å), C(23)···C(70) (3.352(2) Å), C(30)···C(63) (3.372(3) Å) (*x*,*y*,*z*).

Molecular interactions of each molecule of LM-3 were analyzed in detail. Molecule I (Fig. 4a), II (Fig. 4b) and IV (Fig. 4d) were in vicinity to four and molecule III (Fig. 4c) was in vicinity to five neighbouring molecules via N—H···O, C—H···O and π–π stacking interactions. Methyl group hydrogen (H(15A), H(55A), H(35C) and H(75C)) and benzenoid hydrogen's (H(7), H(28), H(48), H(67) and H(68)) were involved in C—H···O interaction. Only *n*-alkylamino hydrogen H(33B) of molecule II showed C—H···O interaction to O(41) of molecule III. When viewed down '*b*'-axis (Fig. 5) the dimers of molecules I, IV and II, III further show π–π stacking

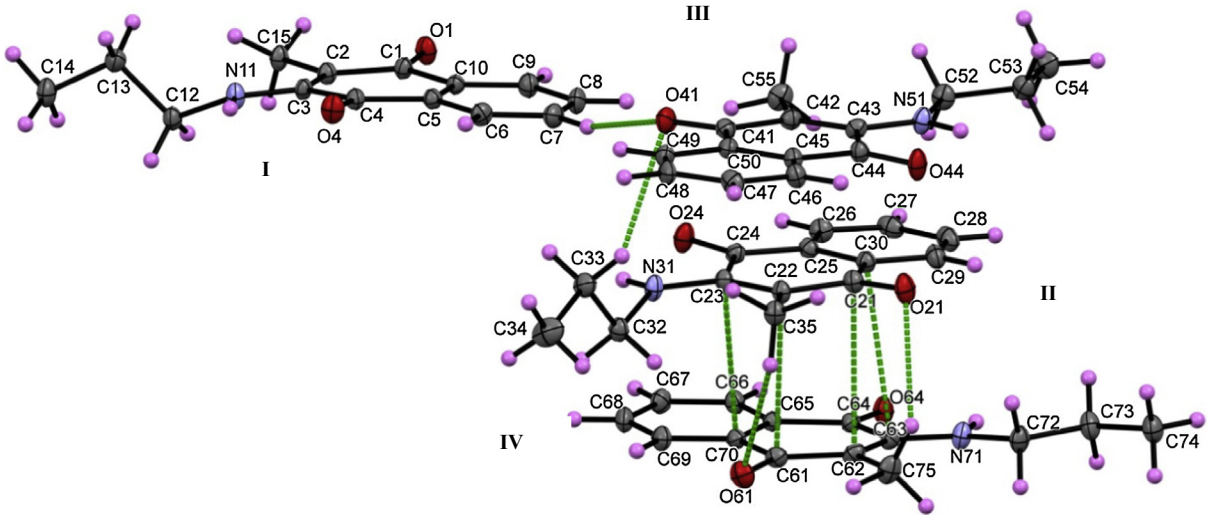

Fig. 3. Asymmetric unit of LM-3.

Table 5
Hydrogen bond geometries for LM-1 and LM-3.

Com	Sr. No	D—H···A	D—H (Å)	H···A (Å)	D···A (Å)	∠D—H···A (°)
LM-1	1	N(11)—H(11)···O(4)$^{(i)}$	0.92 (2)	2.36 (2)	3.060 (1)	133.0 (2)
	2	C(12)—H(12B)···O(4)$^{(i)}$	0.981 (1)	2.527 (1)	3.209 (2)	126.5 (1)
	3	C(13)—H(13A)···O(1)$^{(ii)}$	0.979 (1)	2.593 (1)	3.393 (2)	139.0 (1)
	4	C(8)—H(8)···O(1)$^{(i)}$	0.981 (2)	2.436 (1)	3.360 (2)	163.8 (8)
LM-3	5	N(31)—H(31)···O(24)^{intra}	0.94 (3)	2.14 (3)	2.608 (2)	109.0 (2)
	6	N(51)—H(51)···O(44)^{intra}	0.98 (3)	2.10 (3)	2.599 (2)	110.0 (2)
	7	N(11)—H(11)···O(4)^{intra}	0.92 (3)	2.16 (3)	2.612 (3)	109.0 (2)
	8	N(71)—H(71)···O(64)^{intra}	0.94 (3)	2.14 (3)	2.601 (3)	110.0 (2)
	9	N(11)—H(11)···O(64)$^{(iii)}$	0.92 (3)	2.11 (3)	2.961 (2)	153.0 (2)
	10	N(71)—H(71)···O(4)$^{(iii)}$	0.94 (3)	2.50 (3)	3.405 (2)	162.0 (2)
	11	N(31)—H(31)···O(44)$^{(iv)}$	0.94 (3)	2.071 (3)	2.933 (3)	151.0 (2)
	12	N(51)—H(51)···O(24)$^{(iv)}$	0.98 (3)	2.696 (3)	3.392 (3)	158.0 (2)
	13	C(15)—H(15A)···O(41)$^{(iv)}$	0.980 (2)	2.677 (2)	3.424 (3)	133.3 (1)
	14	C(55)—H(55A)···O(1)$^{(iv)}$	0.981 (2)	2.597 (1)	3.433 (2)	143.2 (1)
	15	C(35)—H(35C)···O(61)$^{(v)}$	0.980 (2)	2.677 (1)	3.464 (2)	137.6 (1)
	16	C(75)—H(75C)···O(21)$^{(v)}$	0.979 (2)	2.586 (2)	3.398 (3)	140.5 (1)
	17	C(7)—H(7)···O(41)$^{(v)}$	0.951 (2)	2.285 (2)	3.211 (3)	164.5 (1)
	18	C(48)—H(48)···O(1)$^{(vi)}$	0.950 (2)	2.474 (3)	3.401 (3)	165.2 (1)
	19	C(28)—H(28)···O(61)$^{(vii)}$	0.950 (2)	2.517 (3)	3.242 (3)	133.2 (1)
	20	C(67)—H(67)···O(21)$^{(iv)}$	0.950 (4)	2.395 (2)	3.074 (3)	128.1 (1)
	21	C(33)—H(33B)···O(41)$^{(v)}$	0.990 (2)	2.696 (2)	3.444 (2)	132.6 (1)

(i) ½−*x*, ½−*y*, −*z*; (ii) 1−*x*, *y*, ½−*z*; (iii) 1 + *x*, −1 + *y*. Z; (iv) −1 + *x*,*y*,*z*; (v) *x*,*y*,*z*; (vi) *x*, −1 + *y*, −1 + *z*, (vii) *x*, 1 + *y*, *z*.

interactions. The ladders like interactions of LM-3 molecules via N—H···O and π–π stacking interactions were illustrated in Fig. 6. The ladders were connected by a unique C—H···O interaction of *n*-alkyl group of molecule II to oxygen of molecule III. There were no interactions observed between molecules I, II and III, IV.

Molecular interactions in LM-1

A molecule of LM-1 (CCDC No. 640771) [8a] crystallizes in monoclinic *C*2/*c* space group and showed dimer via N—H···O and C—H···O interactions of similar ends of oppositely orientated molecules. This interaction is commonly observed in other *n*-alkylamino derivatives of 1,4-naphthoquinones [7]. Each LM-1 molecule was in vicinity to four neighbouring molecules (i) π–π stacked as well as CH···O interaction of C(13-H(13A)···O(1) (1−*x*, *y*, ½−*z*). (ii) forms dimer with oppositely oriented neighbouring molecule by N—H···O (½−*x*, ½−*y*,−*z*) interaction. (ii) Two molecules with C—H···O interaction (½−*x*, ½−*y*, ½−*z*).

π–π stacking interaction are observed to neighbouring alternating molecules of LM-1 and the carbon atoms involved were C(1)···C(2) (3.429(2) Å), C(3)···C(1) (3.398(2) Å), C(3)···C(10) (3.391(2) Å). π–π stacked molecules were also hold by C—H···O interactions of C(2)—CH_3 group. When viewed down '*b*'-axis each (Fig. 7) π–π Stacked polymeric chains were observed to dimeric LM-1 molecules whereas viewed down '*c*' axis a beautiful butterfly like architecture was observed to two pairs of π–π stacked LM-1 molecules (Fig. 7).

Antibacterial activity of LM-1 to LM-8

The antibacterial activity of LM-1 to LM-8 compounds along with vitamin K3 has been evaluated against two bacterial strains viz, *S. aureus* and *P. aeruginosa* by the agar disc diffusion assay and minimum inhibitory concentration assay.

Bacterial strain like *S. aureus* is one of the major resistant pathogens found on the mucous membrane and human skin and extremely adaptable to antibiotic pressure. It was found to be resistant against clinically used Penicillin and Methicillin drugs. While *P. aeruginosa* is a highly prevalent opportunistic pathogen. It is the most common pathogen isolated from patients who have been

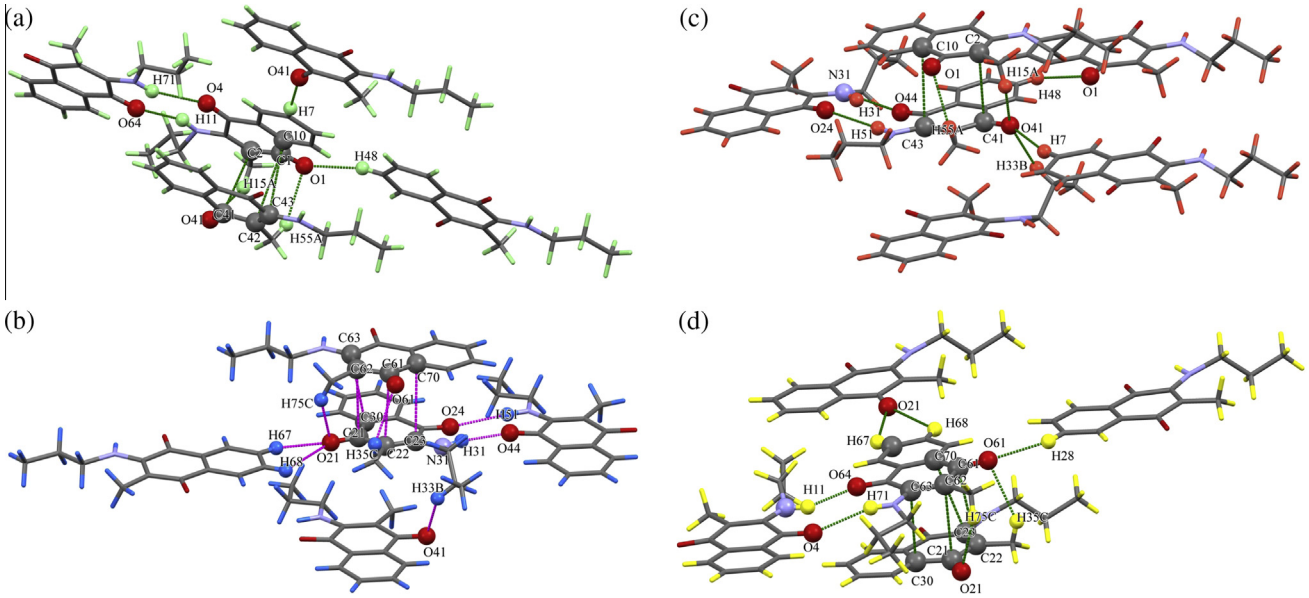

Fig. 4. (a) Neighbouring molecules of I, (b) neighbouring molecules of II, (c) neighbouring molecules of III and (d) neighbouring molecules of IV.

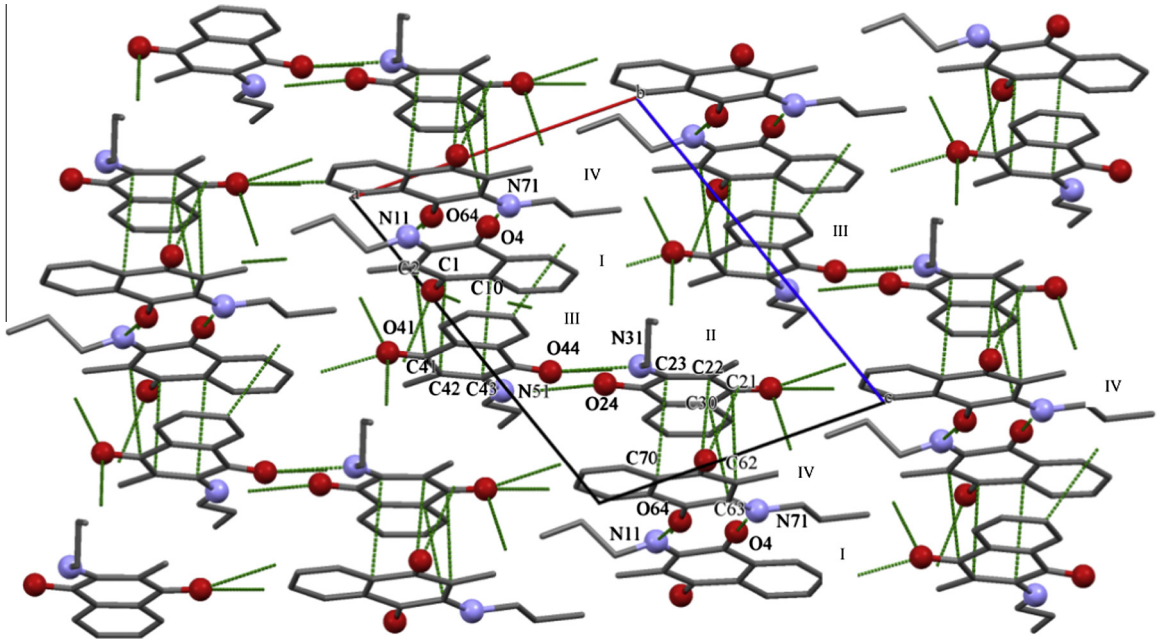

Fig. 5. Hydrogen bonding and π–π stacking interactions in LM-3 down *b*-axis.

hospitalized longer than one week. It is a frequent cause of nosocomial infections such as pneumonia, urinary tract infections and bacteremia especially in patients with compromised host defence mechanisms. One of the most agonizing characteristics of *P. aeruginosa* is its low antibiotic susceptibility. This inactivity may result from lack of prescriber knowledge of specific antimicrobial resistance patterns or suboptimal dosing based on pharmacokinetic and pharmacodynamic properties of each drug class. Hence, there has been a need to synthesis a new class of drug against which these pathogens that do not develop any resistance.

Agar disc diffusion assay of LM-1 to LM-8

The compounds of appropriate concentrations were added on to the disc, dried and sterilized in UV before placing them on the petriplates. The results were presented in Table 6 (Fig. S4 in ESI†) for *P. aeruginosa* and *S. aureus* (in parenthesis). It was observed that all of the compounds showed some activity against the two bacterial strains. In all the cases, there was an increase in the diameter of the clearance zone with increase in the concentration of the compound. To evaluate the minimum concentration required for the inhibition of bacterial growth; the micro dilution method was followed.

Minimum inhibitory concentration assay (MIC)

The minimum inhibitory concentration of vitamin K3 and all compounds against *P. aeruginosa* for *S. aureus* (in parenthesis) were shown in Table 7 (Figs. S5 and S6 in ESI†). It can be seen that most of the compounds showed inhibition only at higher concentration

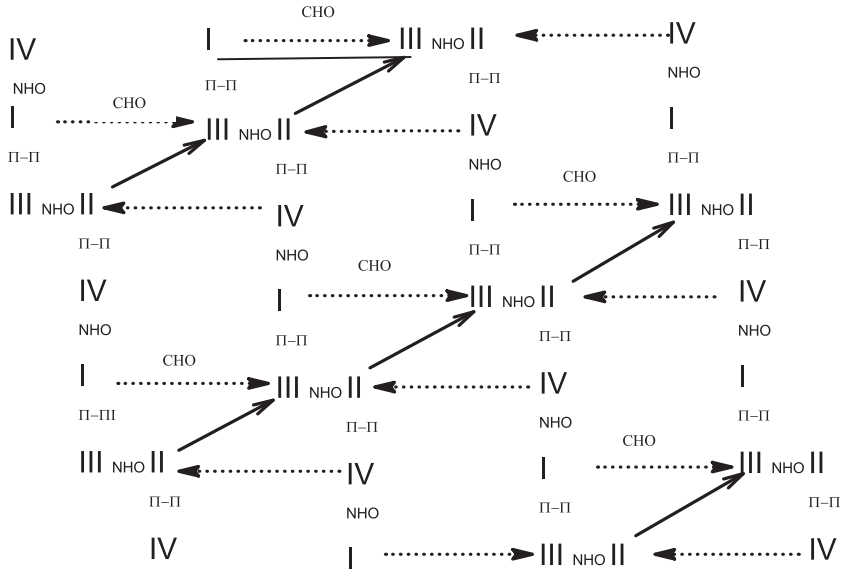

Fig. 6. Illustration of N—H···O (molecules II, III and I, IV) and π–π stacking interactions (I, III and II, IV) of LM-3.

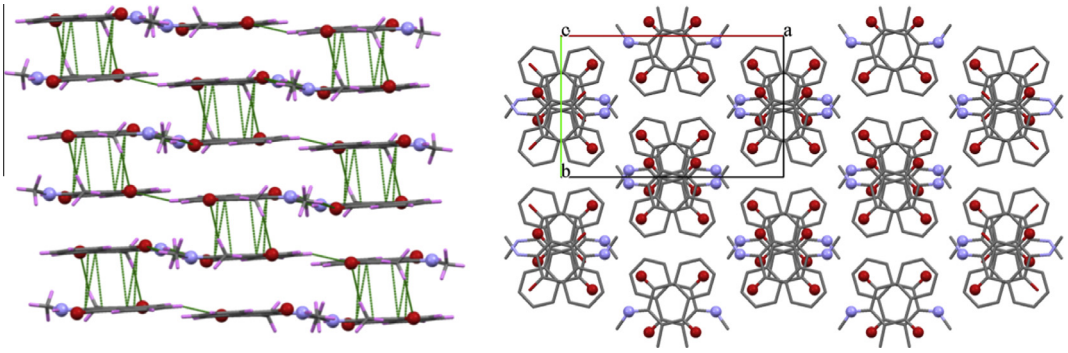

Fig. 7. Molecules of LM-1 showing ladder like alternating π–π stacking interaction between the neighbouring chains down *b*-axis(left) and butterfly like arrangement of LM-1 molecules down *c* axis(right).

Table 6
Results of agar disc diffusion assay of LM-1 to LM-8 on for *Pseudomonas aeruginosa* (*Staphylococcus aureus*).

Compound	Diameter (1 μg/mL)	Of (2 μg/mL)	Clearance (3 μg/mL)	Zone (cm) (5 μg/mL)
Vitamin K3	0.2 (0.6)	0.8 (0.8)[a]	1.4 (1.0)	1.8 (1.2)
LM-1	0.4 (0.5)	0.9 (0.7)	1.2 (0.9)	1.6 (1.1)
LM-2	0.6 (0.6)	0.8 (0.8)	1.0 (0.9)	1.4 (1.4)
LM-3	0.5 (0.7)	0.9 (0.9)	1.3 (1.0)	1.5 (1.2)
LM-4	0.6 (0.6)	0.9 (0.7)	1.1 (0.8)	1.4 (0.9)
LM-5	0.5 (0.4)	0.8 (0.5)	0.9 (0.6)	1.2 (0.8)
LM-6	0.4 (0.2)	0.2 (0.5)	0.9 (0.6)	1.1 (0.9)
LM-7	0.3 (0.3)	0.6 (0.7)	0.8 (0.9)	1.0 (1.0)
LM-8	0.3 (0.4)	0.5 (0.5)	0.7 (0.6)	1.2 (0.8)

[a] For *Staphylococcus aureus*.

against *P. aeruginosa*, however, vitamin K3 showed a good activity at a minimum concentration of 0.156 μg/mL and LM-2 at 0.625 μg/mL.

From Table 7, it is clear that LM-2 is much more effective against *S. aureus*, as it shows good activity at a minimum concentration of 0.3125 μg/mL, whereas the other compounds exhibited good antibacterial activity above 0.625 μg/mL concentration.

The two different assays's showed that all the compounds and vitamin K3 were biologically active. The agar disc diffusion assay showed that the diameter of the clearance zone increased with increase in concentration of the compounds. While the MIC assay gave the minimum concentration required for the inhibition. From the data obtained it can be observed that LM-2 and vitamin K3 showed better activity as compared to the other compounds. The MIC value for LM-2 was 0.625 μg/mL and 0.3125 μg/mL respectively for *P. aeruginosa* and *S. aureus*, (Fig. 8) whereas vitamin K3 showed a minimum concentration of 0.156 μg/mL for *P. aeruginosa.*

Mechanism of biological activity

The antitumor and cytotoxic effects of quinonoid drugs are thought to be mediated through their one-electron or

Table 7
Results of minimum inhibitory concentration assay of LM-1 to LM-8 for *Pseudomonas aeruginosa* and *Staphylococcus aureus*.

Concentration (μg/mL)	Vitamin K3	LM-1	LM-2	LM-3	LM-4	LM-5	LM-6	LM-7	LM-8
0.0024	1.4 (1.1)[a]	1.4 (0.98)	1.4 (0.96)	1.38 (0.97)	1.3 (0.94)	1.4 (0.95)	1.4 (0.96)	1.4 (0.96)	1.4 (0.96)
0.0048	1.38 (0.98)	1.22 (0.88)	1.36 (0.95)	1.36 (0.88)	1.32 (0.83)	1.35 (0.85)	1.36 (0.88)	1.36 (0.84)	1.36 (0.83)
0.0097	1.2 (0.78)	1.36 (0.86)	1.32 (0.97)	1.33 (0.97)	1.34 (0.96)	1.38 (0.92)	1.37 (0.94)	1.32 (0.93)	1.32 (0.91)
0.0195	1.1 (0.63)	1.1 (0.84)	1.12 (0.94)	1.11 (0.94)	1.38 (0.94)	1.37 (0.92)	1.35 (0.92)	1.36 (0.91)	1.36 (0.90)
0.039	0.9 (0.63)	0.82 (0.78)	1.1 (0.98)	1.1 (0.87)	1.36 (0.88)	1.36 (0.89)	1.33 (0.84)	1.1 (0.86)	1.1 (0.85)
0.0781	0.7 (0.62)	0.86 (0.63)	0.93 (0.96)	0.98 (0.78)	1.22 (0.83)	1.22 (0.88)	1.1 (0.75)	0.96 (0.86)	0.98 (0.85)
0.156	0.2 (0.65)	0.85 (0.62)	0.85 (0.99)	0.89 (0.63)	1.11 (0.78)	1.1 (0.74)	1.28 (0.62)	0.97 (0.84)	0.98 (0.84)
0.3125	0.8 (0.64)	0.73 (0.61)	0.76 (0.28)	0.86 (0.54)	0.96 (0.72)	0.97 (0.68	0.96 (0.61)	0.92 (0.73)	0.92 (0.61)
0.625	0.6 (0.62)	0.75 (0.71)	0.23 (0.35)	0.84 (0.42	0.97 (0.51	0.97 (0.71)	0.97 (0.21)	0.91 (0.21)	0.94 (0.26)
1.25	0.7 (0.20)	0.15 (0.64)	0.45 (0.44)	0.15 (0.52)	0.92 (0.31)	0.98 (0.72)	0.96 (0.6)	0.96 (0.61)	0.97 (0.31)
2.5	0.4	0.32	0.55	0.28	0.21	0.62	0.21	0.97	0.97
5	0.3 (0.32)	0.31 (0.42)	0.46 (0.46)	0.32 (0.34)	0.36 (0.51)	0.21 (0.21)	0.31 (0.51)	0.6 (0.72)	0.6 (0.42)

[a] For *Staphylococcus aureus*.

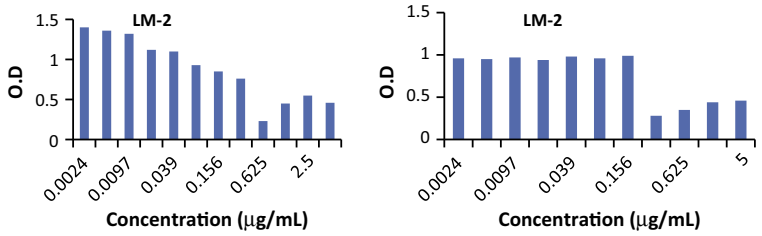

Fig. 8. MIC plots for LM-2 against *Pseudomonas aeruginosa* (left) and *Staphylococcus aureus*(*right*).

two-electron reduction to semiquinone radicals. Most semiquinones rapidly reduce dioxygen to form superoxide anion radical and thus regenerate the quinone. Quinones may, therefore, enter flavoprotein-catalyzed redox cycles with dioxygen which result in the formation of large amounts of $O_2^{-}\cdot$ radical and the oxidation of reduced pyridine nucleotides. The enzymatic or spontaneous dismutation of $O_2^{-}\cdot$ yields H_2O_2 and O_2. Further $O_2^{-}\cdot$ and H_2O_2 can react together, in a process catalyzed by certain metal ions, to form even more deleterious oxygen species such as the hydroxyl radical ($OH^{\cdot}$) by Fenton reaction and singlet oxygen. The flavoprotein-catalyzed redox cycling of quinones in cells would, therefore, quickly lead to conditions of oxidative stress due to excess of the superoxide radical. These oxygen intermediates or reactive oxygen species (ROS) may react directly with DNA or other biomolecules such as proteins and lipids, which leads to cell damage [21–24]. In in vivo, the flavoprotein NAD(P)H which is a quinone-acceptor oxidoreductase, catalyzes the two-electron reduction of quinones to hydroquinones without the formation of semiquinone radical intermediates, whereas NADPH-cytochrome P-450 reductase and NADH-ubiquinone oxidoreductase catalyze the one-electron reduction of quinones to semiquinone radicals. Thus the mechanism of biological activity involves generation of active oxygen species by redox cycling, intercalation between nucleotides in the DNA double helix or alkylation of biomolecules.

Conclusions

Synthesis, characterization and evaluation of antibacterial activity of first eight analogs of *n*-alkylamino derivatives (LM-1 to LM-8) of vitamin K3 has been discussed in this investigation. Molecular structure of LM-3 (propyl derivative) has been determined by single crystal X-ray diffraction and its molecular association with neighbouring molecules were investigated in detail. There were four molecules in asymmetric unit cell of LM-3; they were named as I, II, III and IV. The four molecules differed by torsion angles and bond angles of the plane of quinonoid ring and the N-alkyl chain. Molecules I, IV and II, III formed dimer via N—H···O interaction while there was no molecular association of molecules I and II similarly III and IV in crystal lattice. The ladders of all four molecules of LM-3 are observed via C—H···O, N—H···O and π–π stacking interactions. The ladders were connected by a unique C—H···O interaction of *n*-alkyl group of molecule II to III. The overall interactions of LM-3 are presented in Fig. 9. Molecules of LM-1 also formed dimer and further a polymeric chain of dimers was formed by C—H···O interaction. Neighbouring chains of dimers showed alternatively π–π stacking of molecules.

Pharmacological potential of all compounds has been evaluated against two bacterial strains viz *P. aeruginosa* and *S. aureus*. All the compounds showed activity against the two strains under

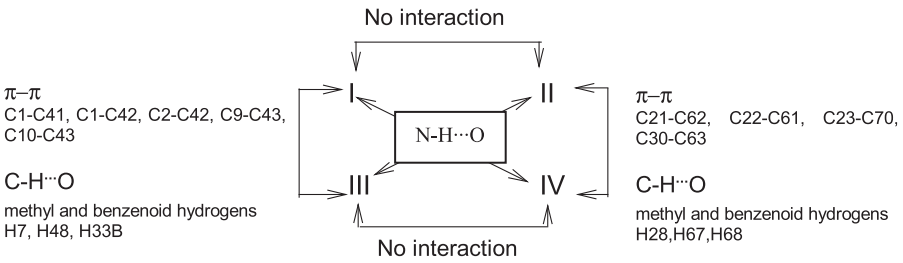

Fig. 9. Overall interactions of LM-3 molecules.

investigation especially; LM-2 was found to be more effective against *P. aeruginosa* and *S. aureus* with minimum inhibitory concentration respectively of 0.625 μg/mL and 0.3125 μg/mL. Probable mechanism of antibacterial activity was discussed.

Acknowledgement

SSG grateful to RGYI scheme of Department of Biotechnology, New Delhi, India for Ref. No. (BT/PR6565/GBD/27/456/2012).

Appendix A. Supplementary material

Supplementary data associated with this article can be found, in the online version, at http://dx.doi.org/10.1016/j.molstruc.2015.01.029.

References

[1] M. Billeter, W. Bolliger, C. Martius, J. Biochem. 340 (1964) 290–303.
[2] R.T. Davidson, A.L. Foley, J.A. Engelke, J.W. Suttie, J. Nutr. 128 (1998) 220–223.
[3] D.W. Lamson, S.M. Plaza, Altern. Med. Rev. 8 (2003) 303–318.
[4] H.H.W. Thijssen, L.M.T. Vervoort, L.J. Schurgers, M.J. Shearer, J. Nutr. 95 (2007) 260.
[5] A. AlRajabi, J. Peterson, S.W. Choi, J. Suttie, S. Barakat, S.L. Booth, J. Chromatogr. Analyt. Technol. Biomed. Life Sci. 878 (2010) 2457–2460.
[6] Z. Liu, T. Li, J. Li, E. Wang, Anal. Chim. Acta 338 (1997) 57–62.
[7] (a) S. Pal, M. Jadhav, T. Weyhermüller, Y. Patil, M. Nethaji, U. Kasabe, L. Kathawate, V. Badireenath Konkimalla, S. Salunke-Gawali, J. Mol. Struct. 1049 (2013) 355–361;
(b) O. Pawar, A. Patekar, A. Khan, L. Kathawate, S. Haram, G. Markad, V. Puranik, S. Salunke-Gawali, J. Mol. Struct. 1059 (2014) 68–74;
(c) S. Salunke-Gawali, O. Pawar, M. Nikalje, R. Patil, T. Weyhermüller, V.G. Puranik, V. Badireenath Konkimalla, J. Mol. Struct. 1056–1057 (2014) 97–103.
[8] (a) H.R. Nasiri, R. Panisch, M.G. Madej, J.W. Bats, C.R.D. Lancaster, H. Schwalbe, Biochim. Biophys. Acta 1787 (2009) 601–608;
(b) M.P. Brun, E. Braud, D. Angotti, O. Mondesert, M. Quaranta, M. Montes, M. Miteva, N. Gresh, B. Ducommun, C. Garabay, Bioorg. Med. Chem. 13 (2005) 4871–4879;
(c) T. Kayshima, M. Mori, R. Mizutani, K. Nishio, K. Kuramochi, K. Tsubaki, H. Yoshida, Y. Mizushina, K. Matsubara, Bioorg. Med. Chem. 18 (2010) 6305–6309;
(d) T. Karunan, N. Mathew, L. Srinivasan, K. Muthuswamy, Drug. Dev. Res. 74 (2013) 216–226.
[9] D.D. Perrin, W.L. Armarego, Purification of Laboratory Chemicals, Pergamon Press, London, 1988. pp 260.
[10] ShelXTL 6.14 Bruker AXS Inc., Madison, WI, USA 2003.
[11] SADABS, Bruker-Siemens Area Detector Absorption and Other Correction, G.M. Sheldrick, University of Göttingen, Germany, 2006, Version 2008/1.
[12] G.M. Sheldrick, SHELX-97 Program for Crystal Structure Solution and Refinement, University of Göttingen, Germany, 1997.
[13] D.W. Cameron, P.M. Scott, J. Chem. Soc. (1964) 5569–5573.
[14] B. Liu, Synth. Commun. 38 (2008) 1201–1211.
[15] K.Y. Chu, J. Griffiths, J. Chem. Soc., Perkin Trans. 1 (1979) 696–701.
[16] K.Y. Chu, J. Griffith, J. Chem. Soc., Perkin Trans. 1 (1978) 1083–1087.
[17] D. Jacquemin, J. Preat, V. Wathelet, E.A. Perpète, Chem. Phys. 11 (2009) 324–332.
[18] E.A. Perpete, C. Lambert, V. Wathelet, J. Preata, Spectrochim. Acta A 68 (2007) 1326–1333.
[19] R. Patil, D. Chadar, D. Chaudhari, J. Peter, M. Nikalje, T. Weyhermüller, S. Salunke-Gawali, J. Mol. Struct. 1075 (2014) 345–351.
[20] (a) M.F. Gross, M.G. Finn, J. Am. Chem. Soc. 116 (1994) 10921–10933;
(b) b) S. Ariel, J. Trotter, Sec. B: Struct. Sci. 44 (1988) 538–544;
(c) K. Kagawa, K. Tokura, K. Uchida, H. Kakushi, T. Shike, H. Nakai, Chem. Pharm. Bull. 40 (1992) 2083–2087;
(d) K. Peters, E.-M. Peters, H.G. von Schnering, G. Bringmann, C. Kehr, R.D. Haller, S. Bar, M.A. Isahakia, S.A. Robertson, Z. Kristallogr. 210 (1995) 290–291;
(e) M. Breton-Lacombe, Acta Crystallogr. 23 (1967) 1016–1024;
(f) J. Vijayalakshmi, S.S. Rajan, R. Srinivasan, Sec. C: Cryst. Struct. Commun. 43 (1987) 2372–2375;
(g) M. Breton, N.B. Chanh, J. Housty, D. Louer, Mol. Cryst. Liq. Cryst. 35 (1976) 261–266.
[21] A. Bolognese, G. Correale, M. Manfra, A. Lavecchia, E. Novellino, S. Pepe, J. Med. Chem. 49 (2006) 5110–5118.
[22] A. Bolognese, G. Correale, M. Manfra, A. Lavecchia, O. Mazzoni, E. Novellino, V. Barone, A. Pani, E. Tramontano, P. La Colla, C. Murgioni, I. Serra, G. Setzu, R. Loddo, J. Med. Chem. 45 (2001) 5205–5216.
[23] S. Jiménez-Alonso, J. Gauasch, A. Estévez-Braun, I. Ratera, J. Veciana, A.G. Ravelo, J. Org. Chem. 76 (2011) 1634–1643.
[24] D.A. Lanfranchi, E. Cesar-Rodo, B. Bertrand, H.-H. Huang, L. Day, L. Johann, M. Elhabiri, K. Becker, D.L. Williams, E. Davioud-Charvet, Org. Biomol. Chem. 10 (2012) 6375–6387.